IETE Journal of Research

ISSN: (Print) (Online) Journal homepage: https://www.tandfonline.com/loi/tijr20

Low-profile Magneto-electric Dipole Antenna

Rekha Ketham , Ayman Abdulhadi Althuwayb & Arvind Kumar

IETE JOURNAL OF RESEARCH
https://doi.org/10.1080/03772063.2021.1873200

Check for updates

Low-profile Magneto-electric Dipole Antenna

Rekha Ketham[1], Ayman Abdulhadi Althuwayb[2] and Arvind Kumar[3]

[1]Madanapalle Institute of Technology and Science, Andhra Pradesh, India; [2]Electrical Engineering Department, College of Engineering, Jouf University (JU), Kingdom of Saudi Arabia; [3]School of Electronics Engineering, Vellore Institute of Technology, Vellore, India

ABSTRACT
Here, a magneto-electric dipole-like antenna is developed for *Ku*-band (12–18 GHz) applications. A low-profile configuration of a magneto-electric dipole antenna has been obtained by the planar arrangement of four shorted patches and L-shaped coax probe. The antenna shows a broad bandwidth response with stable gain and radiation characteristics. The antenna executes an impedance bandwidth between 13.3 and 16.7 GHz with two resonances at 13.9 and 15.6 GHz frequencies. Finally, the antenna has been fabricated and its performance experimentally verified which shows a good agreement with simulated results. The experimental results show −10 dB bandwidth of 11.56%; and peak gain values of 3.9 and 4.6 dBi at 14 and 15 GHz, respectively. On account of the single-layered printed substrate, the proposed antenna can be easily assimilated with associated circuitry.

KEYWORDS
ME dipole antenna; planar antenna; SIW

1. INTRODUCTION

Due to the incredible advances in the electronic/digital transceiver systems, there is an everlasting demand of antenna technologies with the functional characteristics of the broadband operating bandwidth with unidirectional radiation profiles and stable gains. The design of practical low-footprint antennas with broad operational bandwidth remains a consequential subject of the investigation since the commencement of wireless radio transmissions as they have the ability to maneuver a variety of wireless standards simultaneously. Microstrip patch antennas have the merits of low-profile, low-cost, lightweight and easy integration with active circuits. However, the conventional microstrip path antennas possess the narrow operating frequency (−10 dB bandwidth). Conventionally, the bandwidth performance of the antenna is improved by using a stacked structure etc. But, adopting such mechanisms requires a sophisticated fabrication process, and a high cost structure becomes quite complex.

Recently, several magneto-electric dipole antennas (MEDAs) have been investigated and practiced in wireless transmissions, particularly in base stations (BS). They characterize symmetrical radiation patterns, ample bandwidth, minimal cross-polarization, and, remarkably consistent in band radiation gain performance. A novel broadband antenna is developed in [1], MEDA, which comprises one-fourth of the wavelength patch antenna and a half-wavelength electric dipole antenna. This inspired the development of a sequence of enhanced bandwidth characteristics of MEDA in the past decades. The designs of the improved bandwidth of MEDA antennas have been presented in [2–4]. However, the molding and assembling of the copper plane is complex.

However, digitally operated electronic handheld devices need low-profile antennas for planar integration purposes. In [5,6], the printed circuit board (PCB)-based designs are presented. In [5], the antenna has a differential-feeding topology, requires two ports to excite it. The previous designs enhance the functioning bandwidth of the MEDA considerably, but they lead to an intricate structure. Recently, substrate-integrated waveguide (SIW) technology-based antennas have been extensively studied [7–10]. The SIW helps to realize the three-dimensional structure into planar version [11,12]. It maintains merits of its planar complements and has inferior unwanted losses than that of the microstrip, and has been adopted effectively to design high-performance microwave and millimeter-wave RF circuitry [13–17]. However, these antennas do undergo from the limitations of intricate design, including feeding system and mostly proposed at millimeter-wave frequency range. A few advancements on bandwidth enhancement were suggested in [18–21]. Later on, high-profile wideband MEDAs were reported in [22–24] with operating fractional bandwidths of 56, 95.2, and 110%, respectively. But, their 3D volumetric composite metallic structure makes them unfit for many applications in modern wireless communications. Low-profile SIW-based antennas for *Ku*-band application were reported in [25–27].

However, their backed-cavity resonator engages a quite large surface area.

Here, a magneto-electric dipole-like antenna is proposed for Ku-band (12-18 GHz) applications. A single-layered MEDA configuration has been realized with the help of printing technology, by using an arrangement of shorted patches and an L-shaped coax probe. Due to the dual resonance characteristics of design, the antenna displays an enhanced impedance bandwidth of 11.56%. This manuscript is structured as follows: the design, configuration, and parametric study of the proposed antenna are described in Section 2. Section 3 shows the antenna fabrication and validation of results. Finally, it concludes in Section 4.

2. DESIGN, CONFIGURATION, AND ANALYSIS

Figure 1 demonstrates the proposed concept. The radiating element comprises four printed metallic plates, four rows of metal posts, feed, and a ground plane. The L-shaped feed is used to excite the antenna, which consists of a metal strip connected to 50 Ω coaxial line. A pair of half-wave electric dipoles is molded by printed copper plates. The loaded rows of the metallic posts act as magneto dipoles. The diameter of the metallic posts and the pitch distance between the two posts are 0.6 and 0.9, respectively. The dimension of the metallic post and pitch distance are opted, as given in [28,29], so that these posts act effectively as vertical walls without any leakage. As illustrated in Figure 1, the L-shaped feed excites the horizontal plates and vertically loaded posts simultaneously. Detailed antenna parameter information is provided in Table 1.

The development of evolution stages of the proposed antenna design is illustrated in Figure 2. Their corresponding reflection coefficients (S_{11}) are represented in Figure 3. The design of the antenna begins with the horizontally printed four rectangular metallic plates followed by truncation of the two diagonally opposite plates. The S_{11} parameters evidently show that an expansion of impedance bandwidth is realized by tuning the dimensions of the truncated patches. To comprehend the working principle of the antenna, the current densities on the radiating horizontal plates and the aperture of the vertically loaded posts are shown in Figure 4. Here, T is the period of wave cycle at the center frequency of Ku-band

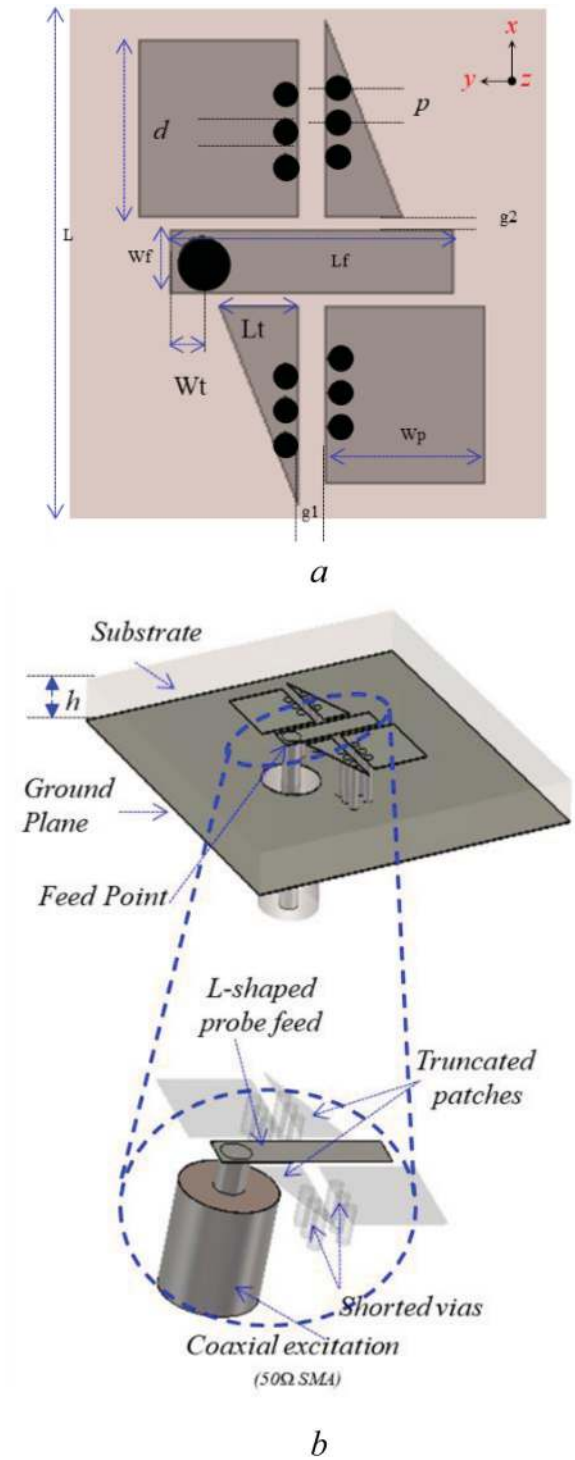

Figure 1: The antenna configuration. (a). The top view and (b) the perspective view

Table 1: The sizes of the antenna dimensions in millimeters.

Parameters	L	W_p	L_p	W_f	L_f	h
Value	24	4.55	4.1	1.6	7.3	1.6
	λ	0.49λ	0.4λ	0.17λ	0.79λ	0.7λ
Parameters	W_t	L_t	p	d	$g1$	$g2$
Value	5.1	2	0.9	0.6	0.7	0.873
	0.55λ	0.21λ	0.9λ	0.6λ	0.7λ	0.87λ

λ, guiding wavelength at the center frequency and f_c = 15 GHz center freq.

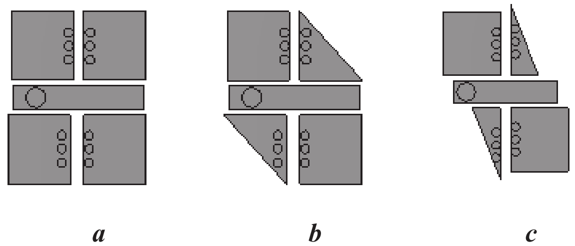

Figure 2: The design evolution of the proposed antenna. (a) Antenna I: with rectangular patches, (b) Antenna II: with truncated rectangular patches, and (c) Antenna III: the proposed design

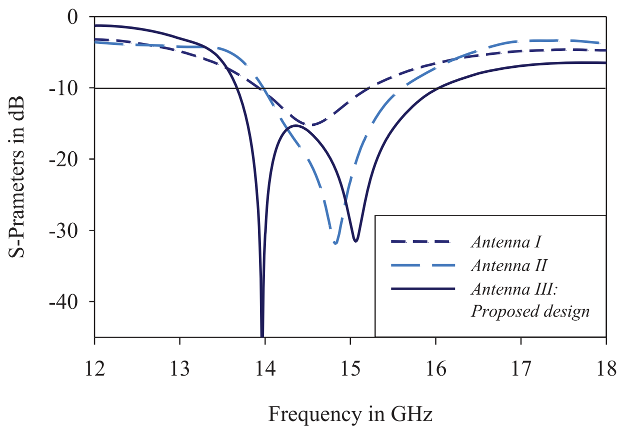

Figure 3: *S*-parameter response for design evolution

(around 15 GHz). At time $t = 0$, the current is concentrated predominantly on the radiating plates, which signifies the electric dipoles are strongly excited. While, at time $t = T/4$, the current is concentrated on the vertical posts, which signifies the magnetic dipoles take the charge. As a result, the electric and magnetic dipoles are excited alternately.

A brief design recommendation of the proposed antenna structure is as follows.

i) Choose the proper thickness of the dielectric substrate, ideally its length should be more than $\lambda/8$. Here, λ is the wavelength at the center frequency of the operating band.
ii) Design two identical planar dipoles which are shorted to the ground by means of metallic posts. Select the sizes of the dipole arm around half of the operating wavelength. The thickness of the metal layer on the dielectric substrate was chosen as 0.035 mm.
iii) Implant the shorting metallic posts as close as to the inner corner of the metallic patches.
iv) Use the L-shaped probe to excite and finely tune L_t, W_t, L_f, and W_f to maximize the impedance bandwidth.

For a better understanding of the operating bandwidth behavior of the antenna, an extensive parametric analysis of *S*-parameter has been executed in Figures 5–8. In each case, only a parameter under consideration is varied, while all others are kept at optimal values, as listed in Table 1. Overall, it can be concluded that the bandwidth performance of the antenna in the desired band is sufficiently stable. Figures 5 and 6 show how the length and width of the rectangular affect the bandwidth matching characteristics. Both parameters are optimized such that the antenna yields maximum bandwidth below −10 dB. Similarly, the parametric study of the length and width of the truncated patch is also performed in Figures 7 and 8, respectively. These parametric studies essentially help to tune the bandwidth and resonant frequencies in the frequency band of interest.

3. FABRICATION AND EXPERIMENTAL STUDY

In order to justify the proposed model and results, a sample of the design was fabricated, as per the dimensions given in Table 1. A single-layered RO4003C substrate of the height of 1.6 mm, with a relative permittivity of 3.55, was used. The manufacturing process of the antenna is performed with the help of a printing circuit technique which realizes copper imprints on the dielectric substrate. The shorting metallic vias are implemented by using printing the through-hole-process (PTH). The reflection coefficients $|S_{11}|$ of the antenna are measured with the help of the Anritsu (Shock-Line MS46122B series) vector network analyser (VNA). The top and bottom views of the fabricated antenna are displayed in Figure 9. The measured and simulated reflection coefficients (S_{11}) are shown in Figure 10. It can be observed that the measured result follows the simulated counterpart with minute deviation, which may be instigated by fabrication/measurement deficits. The proposed design displays a broadband response in Ku-band, as its measured impedance bandwidth is 11.56%, ranging from 13.3 to 16.7 GHz with the dual resonances of 13.9 and 15 GHz. The measurement of the gain of the antenna is performed with the help of the standard horn antenna using the above-mentioned VNA. The simulated and measured frequency-gain characteristics are shown in Figure 11. It can be obviously understood the simulated gain characteristics of the antenna for the entire operating bandwidth are uniform (around 5 dBi). The measured gain values at the frequencies around 14 and 15 GHz are characteristically 3.9 and 5.0 dBi, respectively. The measured gains have fallen down by around 1 dBi as equated to the simulated ones. This inconsistency is generally due to the insertion loss, fabrication and measured errors. Additionally, the simulated versions of total antenna efficiency

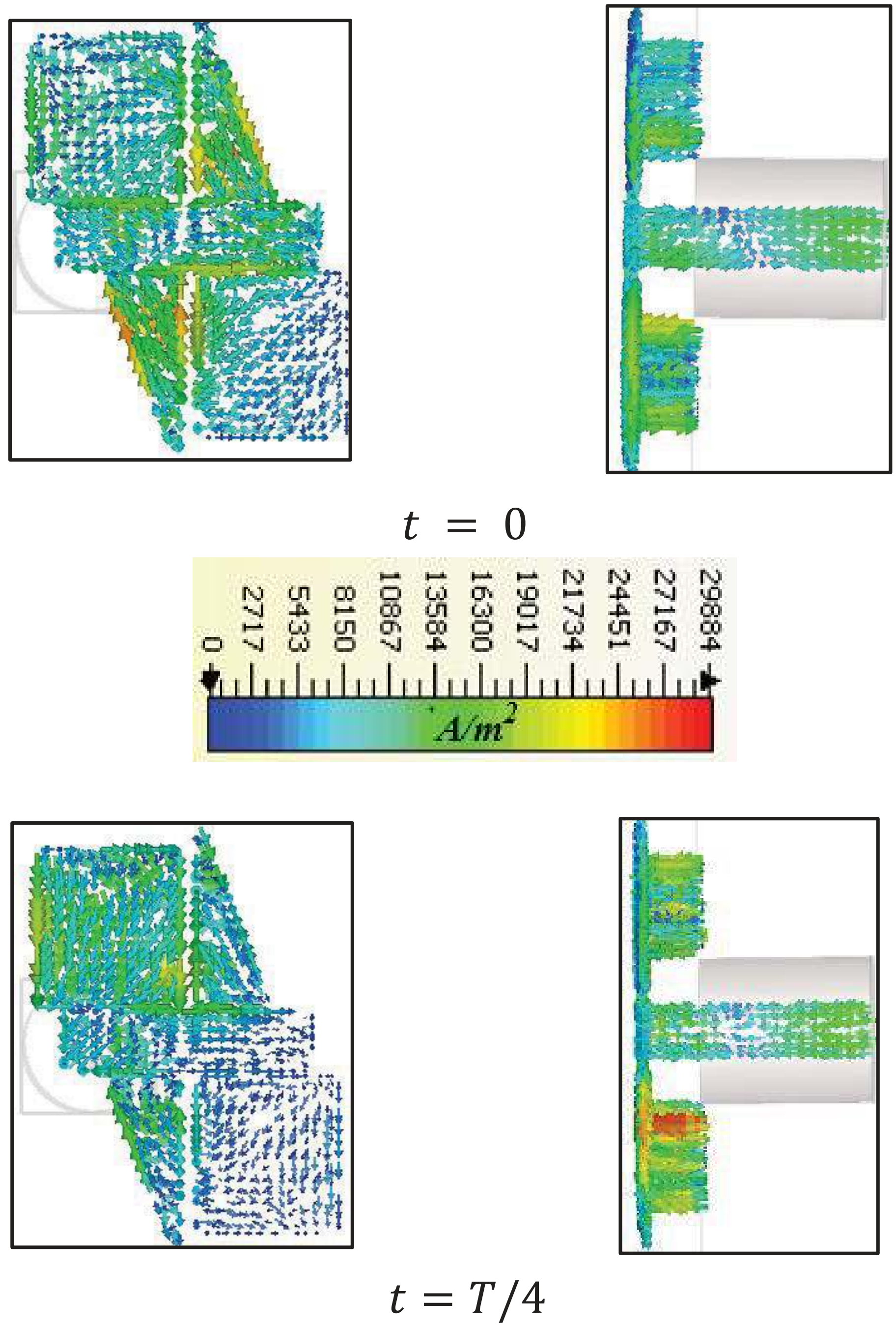

Figure 4: The current density for different time instants

and radiation efficiency are shown in Figure 11, which are better than 90% in the functioning frequency band. The far-field radiation pattern measurements are performed with the help of the test antenna in the anechoic chamber at the distance much more than $\lambda/2\pi$. Figure 12 shows radiation patterns in *yz-plane* and *xz-plane* at the resonant frequencies of around 13.8 and 15 GHz, respectively. Over the operating frequencies, the main beam of the radiation patterns is almost in the broadside direction. Due to the bottom ground plane, the design shows unidirectional radiation patterns. The radiation patterns in the both planes are nearly identical and show a good agreement with simulated results. However, there is a slight deviation from broadside direction, which can be attributed to asymmetry of the antenna around its excitation point or limited substrate thickness. The measured cross-polar radiation levels are better than 10 dB in each case. The measured front-to-back ratio of the proposed antenna is above 12 dB at the resonant frequencies. To highlight the contribution of the present work, a comparison table of the electrical parameter of the proposed antenna with previously works is presented (Table 2).

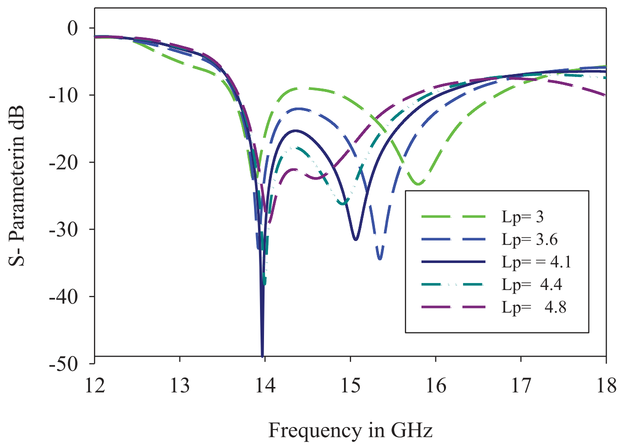

Figure 5: The *S*-parameters: variation in parameter "L_p"

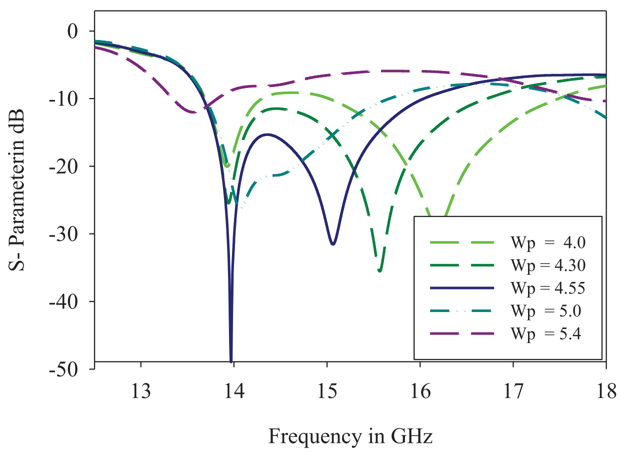

Figure 6: The *S*-parameters: variation in parameter "W_p"

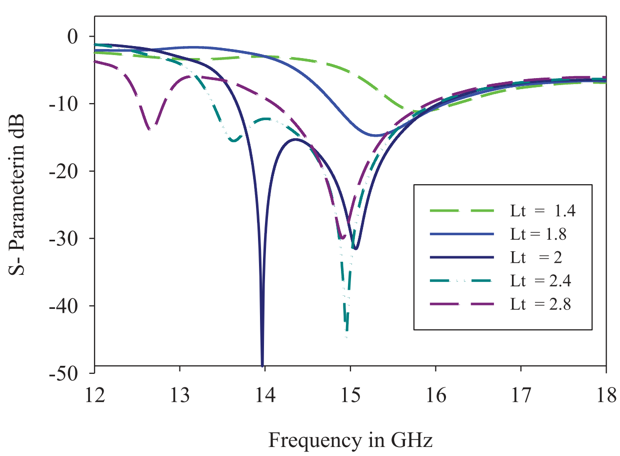

Figure 7: The *S*-parameters: variation in parameter "L_t"

It can be clearly pragmatic that the performance of the proposed work is quite significant while it maintains a quite low profile. It can be perceived that this design keeps relatively smaller printed circuits in terms of overall volume with good radiation performance. The radiation characteristics of the proposed antenna are quite stable. The proposed design possesses a simple configuration and low-heightened substrate (1.57 mm), which

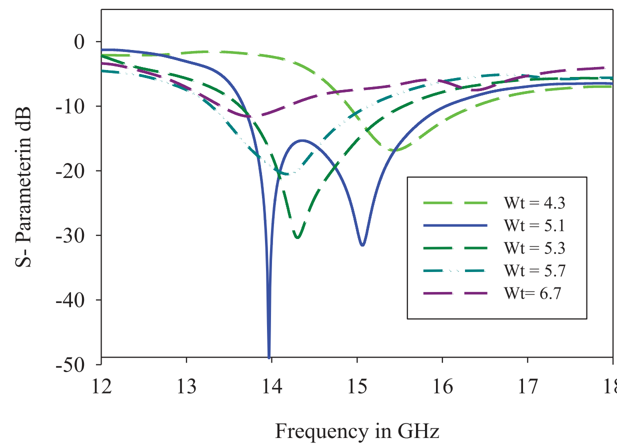

Figure 8: The *S*-parameters: variation in parameter "W_t"

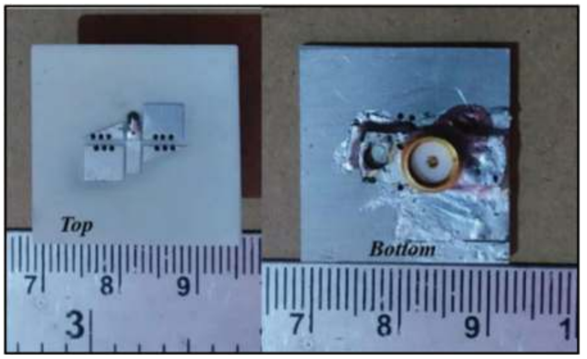

Figure 9: The top and bottom view of the fabricated antenna prototype

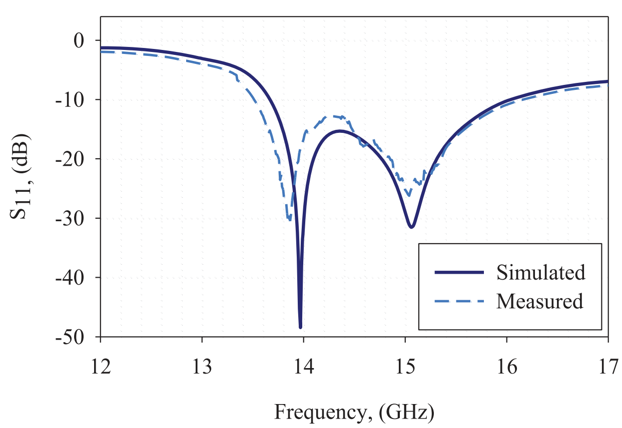

Figure 10: Simulated and measured reflection coefficients (S_{11})

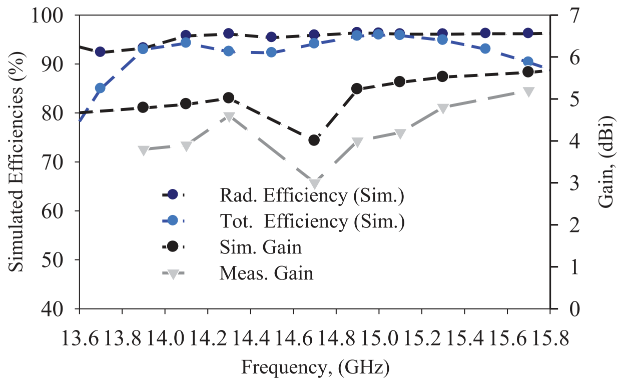

Figure 11: The antenna efficiencies and radiation gain performance

makes it more suitable for a compact and unified digital communication system. Besides, most of the previously reported works emphasize on the millimeter-wave range. The proposed design has a modest arrangement and low profile which makes it better applicant in the microwave frequency range of Ku-band (12–18 GHz) for wireless transmissions, particularly satellite (*Ku*-band) communications/transmissions. The planar magneto-dielectric dipole antenna can find potential applications in different types of wireless communications such as BS for mobile communications, ultra-wideband systems and millimeter-wave radio.

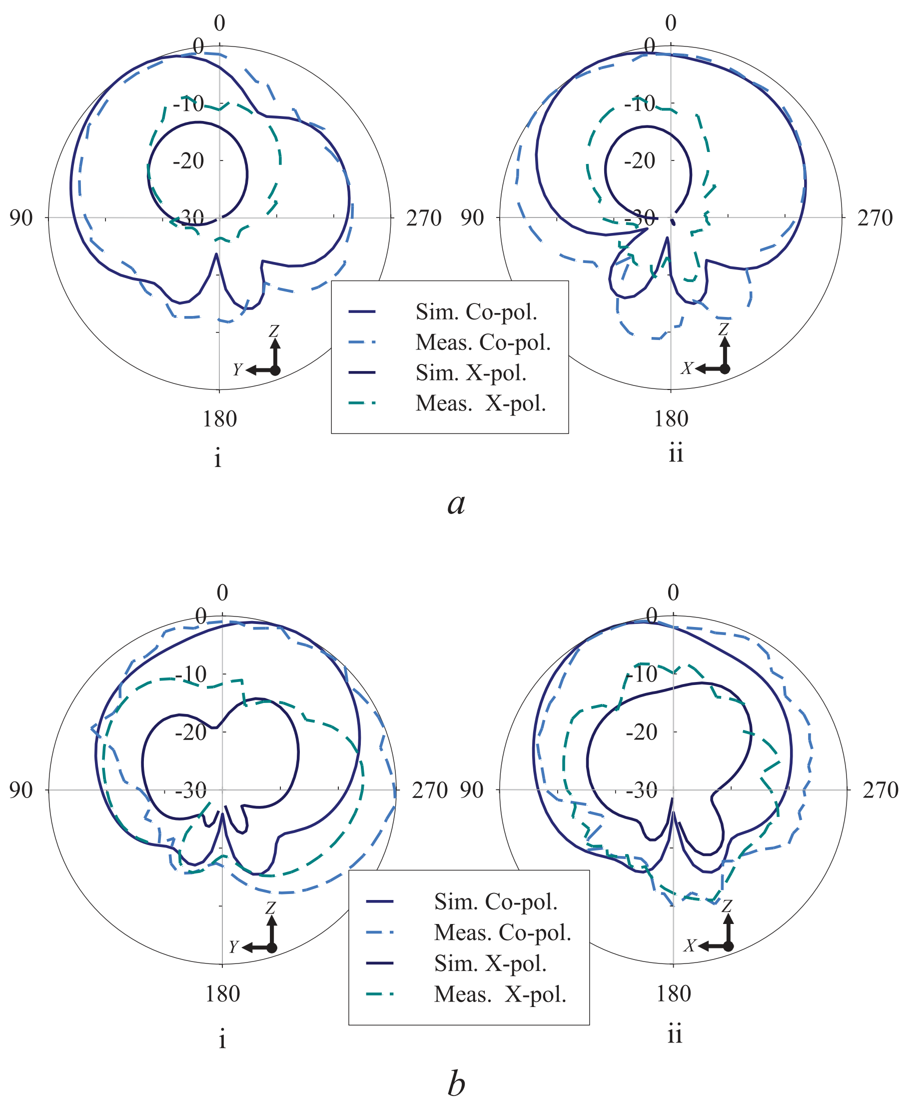

Figure 12: Radiation Profiles at: (a) 13.8 GHz: (i) *yz*-plane and (ii) *xz*-plane and (b) 15 GHz: (i) *yz*-plane and (ii) *xz*-plane.

Table 2: Performance comparison of electrical parameters with previously reported antennas

Ref.	Center freq. and operating frequency band (GHz)	Bandwidth (%)	Height (mm)	Size (in terms of λ)	Gain (dBi)	Dielectric material/air	Configuration type and feed
Here,	15, 13.3–16.7	11.56	1.57	2.2λ × 2.2λ	3.9, 4.6	3.55	Single-layered planar structure, L-shaped probe
[18]	5.5, 4.98–6.01	18.74	1.5	1.07λ × 1.07λ	6.8	2.65	Four-layered structure, complex, L-shaped probe
[19]	14.95, 11.4–18.5	32	3	1.75λ× 1.75λ	11.1	2.2	Planar, high thickness, L-shaped probe
[20]	11.51, 5.63–5.88	4.3	2.4-3.3	2.55λ × 0.459λ	2.4-3.3	2.2	Planar, high thickness, L-shaped probe
[21]	5.52, 5.07–5.95	16	11	1.57λ × 1.57λ	8.2	2.33	Complex, 3D metallic structure, microstrip line
[22]	2.24, 1.62–2.87	56	45.7	2.18 λ × 2.18 λ	5.8–8.9	1, Air	Complex, 3D metallic structure, microstrip line
[23]	3.15, 1.65–4.65	95.2	23	1.26λ × 1.26λ	7.9	1, Air	Complex, 3D metallic structure, microstrip line
[24]	6.84, 3.08–10.6	110	12.4	2.193λ × 1.68λ	8.7 ± 1.9	2.2	Complex, 3D metallic structure, microstrip line
[25]	13.65, 12.7–14.6	11.0	1.57	1.2 λ × 1.63λ	6.0	2.2	SIW-based planar structure, microstrip line
[26]	16.02, 15.55–16.50	5.9	1.57	0.8λ × 2.0λ	6.1	2.2	SIW-based planar structure, microstrip line
[27]	15.46, 14.43–16.49	13.53	1.57	0.77λ × 1.63λ	4.5	2.2	SIW-based planar structure, microstrip line

4. CONCLUSION

A planar MEDA is proposed using a single-layered structure. The design is fabricated and the measured results agree well with the simulations. The antenna shows a wideband response of 11.56% as it operates between 13.5 and 16.18 GHz. The maximum and average gain values in the operating frequency band are around 5.2 and 4.01 dBi, respectively. Moreover, the antenna has the advantages of low-cost manufacturing, lightweight, and compact structure. The design has a single feed and a modest structure which can be scaled for any anticipated frequency. Also, the simulated efficiency is around 90%. With these featured characteristics, the proposed antenna will be appropriate for Ku-band applications.

ACKNOWLEDGMENTS

The authors would like to acknowledge the Rogers Corporation, USA, for providing the substrate.

ORCID

Ayman Abdulhadi Althuwayb http://orcid.org/0000-0001-5160-5016
Arvind Kumar http://orcid.org/0000-0002-9695-4399

REFERENCES

1. K. M. Luk, and H. Wong, "A new wideband unidirectional antenna element," *Int. J. Microw. Opt. Technol*, Vol. 1, no. 1, pp. 35–44, 2006.
2. H. Wong, K.-M. Mak, and K.-M. Luk, "Wideband shorted bowtie patch antenna with electric dipole," *IEEE Trans. Antennas Propag.*, Vol. 56, no. 7, pp. 2098–101, Jul. 2008.
3. L. Ge and K. M. Luk, "A wideband magneto-electric dipole antenna," *IEEE Trans. Antennas Propag.*, Vol. 60, no. 11, pp. 4987–91, Nov. 2012.
4. G. Idayachandran, and R. Nakkeeran, "Compact magneto-electric dipole antenna for LTE femtocell base stations," *Electron. Lett.*, Vol. 52, no. 8, pp. 574–6, 2016.
5. M. J. Li, and K. M. Luk, "A differential-fed magneto-electric dipole antenna for UWB applications," *IEEE Trans. Antennas Propag.*, Vol. 61, no. 1, pp. 92–9, Jan. 2013.
6. L. Ge, and K. M. Luk, "A magneto-electric dipole for unidirectional UWB communications," *IEEE Trans. Antennas Propag.*, Vol. 61, no. 11, pp. 5762–5, Nov. 2013.
7. D. Chaturvedi, and S. Raghavan, "A half-mode SIW cavity-backed semi-hexagonal slot antenna for WBAN application," *IETE. J. Res.*, Vol. 65, no. 5, pp. 582–8, 2019.
8. A. Kumar, "Wideband circular cavity-backed slot antenna with conical radiation patterns," *Microw. Opt. Technol. Lett.*, Vol. 62, no. 6, pp. 2390–7, 2020.
9. M. Saravanakumar, A. Kumar, and S. Raghawan, "Substrate integrated waveguide-fed wideband circularly polarised antenna with parasitic patches," *Def. Sci. J.*, Vol. 69, no. 1, Jan. 2019.
10. A. Kumar, and S. Raghavan, "Bandwidth enhancement of substrate integrated waveguide cavity-backed Bow-tie-complementary-ring-slot antenna using a shorted-via," *Def. Sci. J.*, Vol. 68, no. 2, pp. 197–202, Mar. 2018.
11. D. Chaturvedi, and S. Raghavan, "Compact QMSIW-based antenna with different resonant frequencies depending on loading of metalized vias," *International Journal*

of Microwave and Wireless Technologies, Vol. 11, no. 4, pp. 420–7, May 2019.

12. A. A. Althuwayb, M. J. AlHasan, A. Kumar, and D. Chaturvedi, "Design of halfmode substrate integrated cavity inspired dualband antenna," *Int. J. RF Microw. Comput. Aided Eng.*, e22520, 2020. doi:1002/mmce.22520.

13. A. Kumar, "Design of selfquadruplexing antenna using substrate-integrated waveguide technique," *Microwave Opt. Technol. Lett.*, Vol. 61, pp. 2687–9, 2019.

14. Z.-C. Hao, M. He, K. Fan, and G. Luo, "A planar broadband antenna for E-band gigabyte wireless communication," *IEEE Trans. Antennas Propag.*, Vol. 65, no. 3, pp. 1369–73, 2017.

15. N. Ghassemi, K. Wu, S. Claude, X. Zhang, and J. Bornemann, "Lowcost and high-efficient W-band substrate integrated waveguide antenna array made of printed circuit board process," *IEEE Trans. Antennas Propag.*, Vol. 60, no. 3, pp. 1648–53, 2012.

16. Y. J. Cheng, W. Hong, and K. Wu, "94 GHz substrate integratednmonopulse antenna array," *IEEE Trans. Antennas Propag.*, Vol. 60, no. 1, pp. 121–8, 2012.

17. Y. J. Cheng, Y. X. Guo, and Z. G. Liu, "W-Band large-scale high-gain planar integrated antenna array," *IEEE Trans. Antennas Propag.*, Vol. 62, no. 6, pp. 3370–3, 2014.

18. H. W. Lai, and H. Wong, "Substrate integrated magneto-electric dipole antenna for 5G Wi-Fi," *IEEE Trans. Antennas Propag.*, Vol. 63, no. 2, pp. 870–4, 2015.

19. W. Cao, et al., "Gain enhancement for wideband CP ME-dipole antenna by loading with spiral strip in Ku-band," *IEEE Trans. Antennas Propag.*, Vol. 66, no. 2, pp. 962–966, Feb. 2018.

20. J. Liu, Y. Li, Z. Liang, and Y. Long, "A planar Quasi-magnetic–electric circularly polarized antenna," *IEEE Trans. Antennas Propag.*, Vol. 64, no. 6, pp. 2108–14, June 2016.

21. L. Ge, and K. M. Luk, "A magneto-electric dipole for unidirectional UWB communications," *IEEE Trans. Antennas Propag.*, Vol. 61, no. 11, pp. 5762–5, 2013.

22. L. Ge, X. Yang, D. Zhang, M. Li, and H. Wong, "Polarization-reconfigurable magnetoelectric dipole antenna for 5G Wi-Fi," *IEEE Antennas Wirel. Propag. Lett.*, Vol. 16, pp. 1504–7, 2017.

23. S.-G. Zhou, Z.-H. Peng, G.-L. Huang, and C.-Y.-D. Sim, "Design of a novel wideband and dual-polarized magnetoelectric dipole antenna," *IEEE Trans. Antennas Propag.*, Vol. 65, no. 5, pp. 2645–9, 2017.

24. L. Ge, and K. M. Luk, "A wideband magneto-electric dipole antenna," *IEEE Trans. Antennas Propag.*, Vol. 60, no. 11, pp. 4987–91, 2012.

25. A. Kumar, and S. Raghavan, "Wideband slotted substrate integrated waveguide cavity-backed antenna for Ku-band application," *Microw. Opt. Technol. Lett.*, Vol. 59, no. 7, pp. 1613–9, 2017.

26. T. Zhang, W. Hong, Y. Zhang, and K. Wu, "Design and analysis of SIW cavity backed dual-band antennas with a dual-mode triangular-ring slot," *IEEE Trans. Antennas Propag.*, Vol. 62, no. 10, pp. 5007–16, 2014.

27. A. Kumar, and S. Raghavan, "Broadband SIW cavity-backed triangular-ring-slotted antenna for Ku-band applications," *AEU-Int. J. Electron. Commun.*, Vol. 87, pp. 60–4, 2018.

28. A. Kumar, and M. A. J. Al-Hasan, "A coplanar-waveguide-fed planar integrated cavity backed slotted antenna array using TE33 mode," *Int J RF Microw Comput Aided Eng.*, Vol. 30, no. 10, pp. e22344, 2020.

29. A. Kumar, and S. Raghavan, "A design of miniaturized half-mode SIW cavity backed antenna," in 2016 IEEE Indian Antenna Week (IAW 2016), IEEE, Madurai, India, Jun. 6–10, 2016, pp. 4–7.

AUTHORS

Rekha Ketham received her UG degree from Madanapalle Institute of Technology and Science (MITS), India. She is pursuing her PG in Digital Electronics and Communications Systems in MITS.

Email: rekhaketham96@gmail.com

Ayman A. Althuwayb received the BSc degree (Hons.) in electrical engineering (electronics and communications) from Jouf University, Saudi Arabia, in 2011, the MSc degree in electrical engineering from California State University, Fullerton, CA, USA, in 2015, and the PhD degree in electrical engineering from Southern Methodist University, Dallas, TX, USA, in 2018. He is currently Assistant Professor with the department of electrical engineering at Jouf University, Kingdom of Saudi Arabia.

Email: aaalthuwayeb@ju.edu.sa

Arvind Kumar received the doctorate degree from NIT Trichy in 2019. Currently, he is an assistant professor in Vellore Institute of Technology, Vellore, India. He is an active researcher in areas of substrate-integrated waveguide (SIW)-based circuits and systems, Microwave Integrated Circuits, millimeter wave and THz technologies. Corresponding author.

Email: arvindkr.nitt@gmail.com